



**HAL**  
open science

## Sensing the Molecular Structures of Hexan-2-one by Internal Rotation and Microwave Spectroscopy

Maike Andresen, Isabelle Kleiner, Martin Schwell, Wolfgang Stahl, Ha Vinh  
Lam Nguyen

► **To cite this version:**

Maike Andresen, Isabelle Kleiner, Martin Schwell, Wolfgang Stahl, Ha Vinh Lam Nguyen. Sensing the Molecular Structures of Hexan-2-one by Internal Rotation and Microwave Spectroscopy. *ChemPhysChem*, 2019, 20, pp.2063-2073. 10.1002/cphc.201900400 . hal-03182567

**HAL Id: hal-03182567**

**<https://hal.u-pec.fr/hal-03182567v1>**

Submitted on 26 Mar 2021

**HAL** is a multi-disciplinary open access archive for the deposit and dissemination of scientific research documents, whether they are published or not. The documents may come from teaching and research institutions in France or abroad, or from public or private research centers.

L'archive ouverte pluridisciplinaire **HAL**, est destinée au dépôt et à la diffusion de documents scientifiques de niveau recherche, publiés ou non, émanant des établissements d'enseignement et de recherche français ou étrangers, des laboratoires publics ou privés.

# Sensing the Molecular Structures of Hexan-2-one by Internal Rotation and Microwave Spectroscopy

Maike Andresen,<sup>[a][b]</sup> Isabelle Kleiner,<sup>[b]</sup> Martin Schwell,<sup>[b]</sup> Wolfgang Stahl,<sup>[a]</sup> and Ha Vinh Lam Nguyen<sup>\*[b]</sup>

**Abstract:** Using two molecular jet Fourier transform spectrometers, the microwave spectrum of hexan-2-one, also called methyl *n*-butyl ketone, was recorded in the frequency range from 2 to 40 GHz. Three conformers were assigned and fine splittings caused by the internal rotations of the two terminal methyl groups were analyzed. For the acetyl methyl group  $\text{CH}_3\text{COC}_3\text{H}_6\text{CH}_3$ , the torsional barrier is  $186.9198(50)\text{ cm}^{-1}$ ,  $233.5913(97)\text{ cm}^{-1}$ , and  $182.2481(25)\text{ cm}^{-1}$  for the three observed conformers, respectively. The value of this parameter could be linked to the structure of the individual conformer, which enabled us to create a rule for predicting the barrier height of the acetyl methyl torsion in ketones. The very small splittings arising from the internal rotation of the butyl methyl group  $\text{CH}_3\text{COC}_3\text{H}_6\text{CH}_3$  could be resolved as well, yielding the respective torsional barriers of  $979.99(88)\text{ cm}^{-1}$ ,  $1016.30(77)\text{ cm}^{-1}$ , and  $961.9(32)\text{ cm}^{-1}$ .

## 1. Introduction

Internal rotation is one of the fundamental effects observed in microwave spectroscopy. This large amplitude motion (LAM) often complicates the spectra by causing each rotational transition to split into multiplets. A solid understanding of the phenomenon and its effects is often necessary to analyze the microwave spectra of a molecule and consequently to determine its gas-phase structure. For a typical type of LAM, internal rotation, the torsional barrier is an important parameter that can be linked to the functional group in many molecular classes. For example, the torsional barrier of the methoxy methyl group in methyl alkanoates has always been around  $420\text{ cm}^{-1}$ , as in the cases of methyl acetate ( $424.581(56)\text{ cm}^{-1}$ ),<sup>[1]</sup> methyl propionate ( $429.324(23)\text{ cm}^{-1}$ ),<sup>[2]</sup> and the two conformers of methyl butyrate ( $419.447(59)\text{ cm}^{-1}$  for the  $\text{C}_1$  conformer and  $420.155(71)\text{ cm}^{-1}$  for the  $\text{C}_s$  conformer).<sup>[3]</sup> Systematic studies on  $\alpha,\beta$ -saturated acetates also show that the torsional barrier of the acetyl methyl group is always close to  $100\text{ cm}^{-1}$ . Examples are methyl acetate,<sup>[1]</sup> ethyl acetate,<sup>[4]</sup> *n*-propyl acetate,<sup>[5]</sup> three conformers of *n*-butyl acetate,<sup>[6]</sup> two conformers of *n*-pentyl acetate,<sup>[7]</sup> *n*-hexyl acetate,<sup>[8]</sup> and allyl acetate.<sup>[9]</sup> Even if the alkyl chain is branched as in isopropyl acetate<sup>[10]</sup> and isoamyl acetate,<sup>[11]</sup> the barrier

height seems to be almost unaffected. It is plausible that conjugation within the ester group is responsible for this relatively low barrier of  $100\text{ cm}^{-1}$ .

Ketones are some of the most often found compounds in nature and widely used throughout organic chemistry. Therefore, a deep knowledge about the ketone structures is desirable to understand the origin of their functions in chemical reactions. For this purpose, microwave spectroscopy can be a helpful tool, as shown in the structural studies on trifluoroacetone<sup>[12]</sup>, acetyl acetone,<sup>[13]</sup> and hexafluoroacetylacetone,<sup>[14]</sup> which provided insights into the keto-enol tautomerism of these molecules. Some ketones with a conjugated double bond system such as methyl vinyl ketone,<sup>[15]</sup> as well as the cyclic ketones acetophenone,<sup>[16]</sup> phenyl acetone,<sup>[17]</sup> benzophenone,<sup>[18]</sup> 2-indanone,<sup>[19]</sup> diketopiperazine,<sup>[20]</sup> and fenchone<sup>[21]</sup> have also been investigated. In addition, ketone complexes with water may provide a potential field of interest with the pioneer works on cyclobutanone-water<sup>[22]</sup> and cyclohexanone-water.<sup>[23]</sup>

There are also some microwave spectroscopic studies on ketones with LAM(s) reported in the literature, i.e. methyl isobutyl ketone<sup>[24]</sup> and methyl neopentyl ketone,<sup>[25]</sup> or some unsaturated ketones such as allyl acetone,<sup>[26]</sup> methyl vinyl ketone,<sup>[15]</sup> and 2-acetyl-5-methylfuran.<sup>[27]</sup> The torsional barrier height of the acetyl methyl group in these ketones varies in a wide range of about  $170\text{ cm}^{-1}$  to  $440\text{ cm}^{-1}$ . While the barrier appears to depend strongly on the substitution on the other side of the carbonyl group, no conclusive trend could be drawn.

We recently started a systematic investigation on linear methyl alkyl ketones which contains studies on ethyl methyl ketone<sup>[28]</sup> and methyl *n*-propyl ketone<sup>[29]</sup> to better understand and explain the difference in the barrier height of the acetyl methyl group in ketones. To continue this series, we report here the results for the torsional barriers determined from the microwave spectrum of methyl *n*-butyl ketone (MBK), also called hexan-2-one. The experimental study is supplemented by quantum chemistry.

MBK (see Figure 1) is a volatile, colorless liquid used in paint and solvents.<sup>[30]</sup> In nature, it is found as a pheromone component in bee glands.<sup>[31],[32]</sup> Pheromones are chemical substances which convey information and transfer signals between insects (e.g. attack triggers, territory markers, and sex fragrances).<sup>[33]</sup> In bees, pheromones are often composed of several tens of different chemical compounds, which are usually volatile molecules such as short alcohols, esters, and ketones.<sup>[34]</sup> Since pheromones are detected in olfactory receptors, an analysis of their gas-phase structures and conformational orientations might be a step towards the understanding of complex receptor-odorant interactions.

Not only the acetyl methyl group  $\text{CH}_3\text{CO}-$ , but also the methyl group located at the end of the butyl chain, hereafter called the butyl methyl group  $-\text{C}_3\text{H}_6\text{CH}_3$ , undergoes internal rotation. Therefore, each rotational transition splits into five torsional species, called  $(\sigma_1\sigma_2) = (00), (01), (10), (11),$  and

[a] M. Andresen M. Sc., Prof. Dr. W. Stahl  
Institute of Physical Chemistry, RWTH Aachen University  
Landoltweg 2, D-52074 Aachen, Germany

[b] M. Andresen M. Sc., Dr. I. Kleiner, Prof. Dr. M. Schwell, Dr. H. V. L. Nguyen\*  
Laboratoire Interuniversitaire des Systèmes Atmosphériques (LISA),  
CNRS UMR 7583, Université Paris-Est Créteil, Université de Paris,  
Institute Pierre Simon Laplace  
61 avenue du Général de Gaulle, F-94010 Créteil, France  
\*E-mail: lam.nguyen@lisa.u-pec.fr

(12),<sup>[35]</sup> which correspond to the AA, AE, EA, EE, and EE\* species, respectively, in Dreizler's notation<sup>[36]</sup> or the respective A, E1, E2, E3, and E4 species using the permutation-inversion formalism of the  $G_{18}$  group.<sup>[37]</sup> The numbers  $\sigma = 0, 1, 2$  represent the three symmetry species A,  $E_a$ ,  $E_b$  of the  $C_3$  group, respectively. In the case of MBK,  $\sigma_1$  refers to the acetyl methyl group,  $\sigma_2$  to the butyl methyl group.

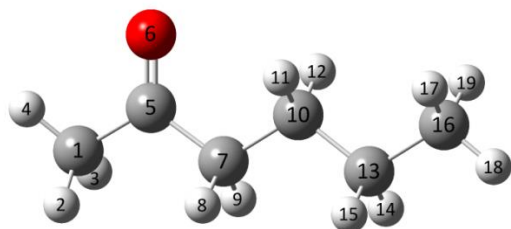


**Figure 1.** Atom numbering of methyl *n*-butyl ketone. The hydrogen atoms are color coded in white, the carbon atoms in gray, and the oxygen atom in red.

The remainder of this paper is divided into sections dealing with: (2) the conformational landscape of MBK obtained by quantum chemistry and theoretical results on the internal rotations of both methyl groups, (3) microwave spectroscopy with spectral assignments and fits, and (4) a brief discussion of our theoretical and experimental results.

## 2. Quantum Calculations

### 2.1. Geometry Optimizations

A total of 27 starting geometries of MBK were created by varying each of the dihedral angles  $\theta_1 = \angle(C_1, C_5, C_7, C_{10})$ ,  $\theta_2 = \angle(C_5, C_7, C_{10}, C_{13})$ , and  $\theta_3 = \angle(C_7, C_{10}, C_{13}, C_{16})$  (for atom numbering, see Figure 1) to  $180^\circ$ ,  $60^\circ$  and  $-60^\circ$ . Changing the dihedral angles  $\alpha_1 = \angle(H_2, C_1, C_5, C_7)$  and  $\alpha_2 = \angle(C_{10}, C_{13}, C_{16}, H_{18})$  corresponds to the internal rotation of the acetyl methyl and the butyl methyl group, respectively, and does not lead to new conformational isomers. Using the *Gaussian09* package,<sup>[38]</sup> the starting geometries were optimized at the MP2/6-311++G(d,p) level of theory to local energy minima, yielding 11 different conformers, each of which exists as an enantiomeric pair. Frequency calculations confirmed that all conformers obtained refer to local minima rather than saddle points. To determine the energetically most favorable conformers, not only the calculated electronic energies but also the zero-point energies (ZPE) were considered. The energies relative to that of the lowest energy conformer, rotational constants, dipole moment components, and optimized dihedral angles are summarized in Table 1. The angles between the principal axes of inertia and the internal rotor axes are given in Table S1 in the Supporting Information (SI).

The MP2/6-311++G(d,p) level of theory was chosen, because it had predicted rotational constants which were in good agreement with the experimental ones in many previous studies.<sup>[39]-[42]</sup> However, since all assignment attempts using the rotational constants predicted at this level of theory as initial values failed (see Section 3.1.), this level turns out to be not adequate in the case of MBK. This observation is consistent with the fact that our studies on the similar molecule methyl propyl ketone have shown the same problems.<sup>[29]</sup> Therefore, the 11

conformers were reoptimized at the B3LYP/6-311++G(d,p) level of theory with the results given in Table 2. The order in energy of the conformers obtained from calculations with the MP2 and the B3LYP method is very different. The structures of the three energetically most favorable conformers obtained with the latter method, called conformer I, II, and III, are illustrated in Figure 2, since they are the conformers eventually identified in the experimental spectrum (see section 3). Their Cartesian coordinates are given in Table S2 of the SI.

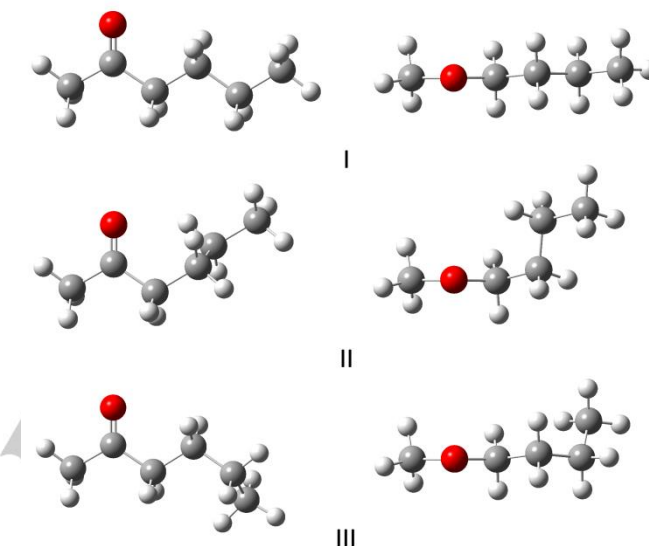


**Figure 2.** Geometries of the three energetically most favorable conformers of methyl butyl ketone optimized at the B3LYP/6-311++G(d,p) level of theory. Left hand side: view on the C-(C=O)-C plane. Right hand side: view along the O=C bond.

Conformer I with a straight butyl chain seems to possess  $C_s$  symmetry, but the dihedral angles optimized at the MP2 and B3LYP levels shown in Table 1 and 2 reveal that the whole butyl group is slightly tilted out of the C-(C=O)-C plane by an angle of about  $10^\circ$  ( $\theta_1 = 169.4^\circ$ ) and  $5^\circ$  ( $\theta_1 = 174.5^\circ$ ), respectively. The same phenomenon could be observed in many other aliphatic ketones, as for example in diethyl ketone,<sup>[43]</sup> pinacolone,<sup>[44]</sup> and methyl neopentyl ketone<sup>[25]</sup> with respective tilt angles of approximately  $12^\circ$ ,  $16^\circ$ , and  $10^\circ$ . Moreover, this tilt-distorted  $C_s$  structure, hereafter called "pseudo- $C_s$ ", is also found for the "straight" conformers of the shorter linear methyl alkyl ketones, methyl ethyl ketone<sup>[28]</sup> ( $9^\circ$ ) and methyl propyl ketone<sup>[29]</sup> ( $10^\circ$ ). This will be further discussed in Section 4.1.

In conformer II, the  $\gamma$ -carbon  $C_{13}$  (for atom numbering, see Figure 1) is in a nearly synclinal position with respect to the C-(C=O)-C plane. The symmetry of this conformer is  $C_1$  and curiously, it contains the  $C_1$  conformer of methyl propyl ketone<sup>[29]</sup>, as a sub-structure. In this comparison, the alkyl chain of MBK is by one  $CH_2$  group longer and the supplementary carbon atom is added at the end of the propyl group of methyl propyl ketone in an antiplanar position ( $\theta_3 \approx 180^\circ$ ). This has also been observed for a series of microwave spectroscopic studies on *n*-alkyl acetates and methyl alkynoates.<sup>[1]-[8]</sup>

Finally, in conformer III only the butyl methyl group is bent to a synclinal position. Interestingly, for the dihedral angles  $\theta_1$ , the values of  $171.1^\circ$  and  $173.1^\circ$  calculated with the MP2 and B3LYP levels, respectively, are similar to those found for conformer I. This indicates that conformer III also exhibits a

“pseudo- $C_s$ ”-like environment in the vicinity of the carbonyl group, as will be further explored in Section 4.2.

## 2.2. Basis Set Variation

Because all assignment attempts using the rotational constants predicted by our most frequently used level of theory MP2/6-311++G(d,p) have failed (see Section 3.1.), the geometry optimizations were redone for conformer I-III at different levels of theory, including Grimme’s dispersion correction,<sup>[45]</sup> to achieve a better agreement between the predicted and experimental value. The results are summarized in Table S3–S5 in the SI.

## 2.3. Internal Rotation

MBK contains two internal rotors, the acetyl methyl group and the butyl methyl group. To calculate the barriers to the internal rotation of these two groups at the MP2/6-311++G(d,p) and B3LYP/6-311++G(d,p) level of theory, the respective dihedral angles  $\alpha_1 = \angle(H_2, C_1, C_5, C_7)$  and  $\alpha_2 = \angle(C_{10}, C_{13}, C_{16}, H_{18})$  were fixed to values in  $10^\circ$  increments. All other geometry parameters were allowed to relax during the optimizations. Due to the symmetry of the methyl group, a rotation of  $120^\circ$  was sufficient. The resulting energies were then parameterized with a one-dimensional Fourier expansion. The coefficients of this expansion are given in Table S6 and S7 in the SI.

### 2.3.1. Acetyl Methyl Group

Only for conformer II, an almost pure  $V_3$  potential is obtained, as illustrated in the upper trace of Figure 3, even though higher order potential terms are needed because the potential curve is not entirely symmetric. This strange shape can be explained by the oscillation of the entire butyl group of up to  $20^\circ$  upon the acetyl methyl rotation (see the lower trace of Figure 3). The MP2 and B3LYP methods yield quite different barrier heights of  $230.1 \text{ cm}^{-1}$  and  $168.7 \text{ cm}^{-1}$ , respectively.

Figures 4 and 5 depict the potential energy curves obtained for conformer I and III, all of which show three double minima. These double minima are also caused by the coupling between the motions of the whole butyl chain and the acetyl methyl group. To look closer at the minima, the dihedral angle  $\alpha_1 = \angle(H_2, C_1, C_5, C_7)$  was varied in finer steps of  $1^\circ$  in the range of  $\pm 20^\circ$  around a local maximum, as shown in the insets of Figure 4 and 5. For conformer I, there is a significant  $V_6$  contribution leading to a local barrier dividing the double minima with a value of  $18.1 \text{ cm}^{-1}$  calculated with the MP2 method, which is clearly more significant than the value of  $1.4 \text{ cm}^{-1}$  obtained with the B3LYP method. Here, the double minima refer to the two enantiomers of conformer I. The respective global barrier height is  $147.6 \text{ cm}^{-1}$  or  $115.5 \text{ cm}^{-1}$ .

For conformer III, the barrier values of  $148.7 \text{ cm}^{-1}$  (MP2) and  $119.0 \text{ cm}^{-1}$  (B3LYP), respectively, are very similar to those of conformer I. However, the two pits of the double minimum are not equivalent and therefore do not refer to an enantiomeric pair. Thus overall, there are three global (conformer III<sub>a</sub>) and three local minima (conformer III<sub>b</sub>) (see the inset of Figure 5). It is difficult to decide which geometry corresponds to the real global energy minimum, because the results calculated with the MP2 and B3LYP methods are contradictory. The respective dihedral angles  $\theta_1$ ,  $\theta_2$  and  $\theta_3$  optimized with the MP2 method are  $-168.6^\circ$ ,  $176.4^\circ$  and  $63.2^\circ$  for conformer III<sub>a</sub> and  $171.1^\circ$ ,  $174.0^\circ$  and  $62.8^\circ$  for conformer III<sub>b</sub>. A significant  $V_6$  contribution is observed with both methods, which again correlates to an oscillation of the entire butyl group of up to  $25^\circ$  upon the acetyl methyl rotation (see the lower trace of Figure 5).

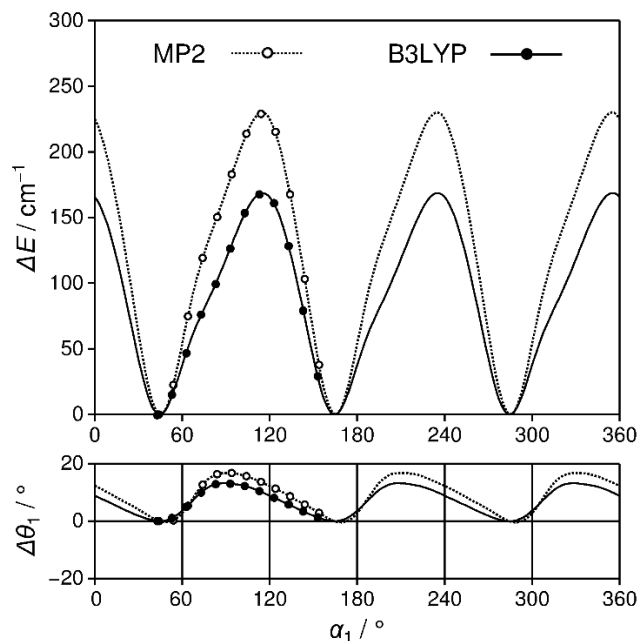


**Figure 3.** Upper trace: Potential energy curve calculated at the MP2/6-311++G(d,p) and B3LYP/6-311++G(d,p) level of theory obtained by rotating the acetyl methyl group of conformer II of methyl butyl ketone. The energies are given relative to the lowest energy conformations. Lower trace: Oscillation of the butyl group visualized by changes in the dihedral angle  $\theta_1 = \angle(C_1, C_5, C_7, C_{10})$  relative to the values  $\theta_1 = 161.2^\circ$  (MP2) and  $\theta_1 = 166.2^\circ$  (B3LYP) of the fully optimized structures.

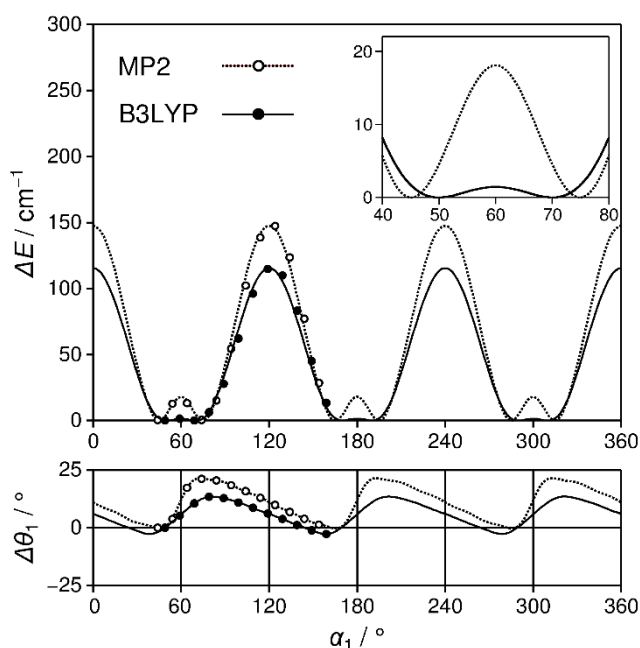


**Figure 4.** Upper trace: Potential energy curve calculated at the MP2/6-311++G(d,p) and B3LYP/6-311++G(d,p) level of theory obtained by rotating the acetyl methyl group of conformer I of methyl butyl ketone. The energies are given relative to the lowest energy conformations. Inset: Enlarged scale for the region between  $\alpha_1 = 40^\circ$  and  $80^\circ$ . Lower trace: Oscillation of the butyl group visualized by changes in the dihedral angle  $\theta_1 = \angle(C_1, C_5, C_7, C_{10})$  relative to the values  $\theta_1 = 169.4^\circ$  (MP2) and  $\theta_1 = 174.5^\circ$  (B3LYP) of the fully optimized structures.

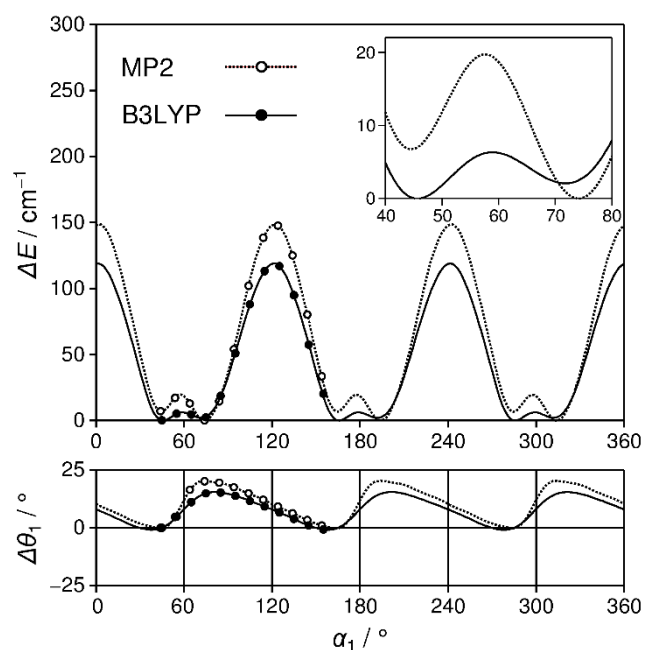


**Figure 5.** Upper trace: Potential energy curve calculated at the MP2/6-311++G(d,p) and B3LYP/6-311++G(d,p) level of theory obtained by rotating the acetyl methyl group of conformer III of methyl butyl ketone. The energies are given relative to the lowest energy conformations. Inset: Enlarged scale for the region between  $\alpha_1 = 40^\circ$  and  $80^\circ$ . Lower trace: Oscillation of the butyl group visualized by changes in the dihedral angle  $\theta_1 = \angle(C_1, C_5, C_7, C_{10})$  relative to the values  $\theta_1 = 171.1^\circ$  (MP2) and  $\theta_1 = 173.1^\circ$  (B3LYP) of the fully optimized structures.

In summary, the barrier to the internal rotation of the acetyl methyl group is estimated to be about  $150 - 250 \text{ cm}^{-1}$ , which is in agreement with observations from previous studies on linear methyl alkyl ketones.<sup>[28],[29]</sup> Torsional splittings in the order of several MHz up to some GHz are expected in the experimental spectrum for molecules featuring similar barrier heights.

### 2.3.2. Butyl Methyl Group

The potential energy curves of the butyl methyl group, as illustrated in Figure S1 in the SI, have a normal three-fold shape with a nearly pure  $V_3$  potential. The barrier height is always around  $1000 \text{ cm}^{-1}$ , as it is also the case for ethyl chloride.<sup>[46]</sup> The values predicted at the MP2/6-311++G(d,p) level of theory are  $1057.6 \text{ cm}^{-1}$ ,  $1067.6 \text{ cm}^{-1}$ , and  $995.5 \text{ cm}^{-1}$  for conformers I-III, respectively. The respective values predicted at the B3LYP/6-311++G(d,p) level are  $994.6 \text{ cm}^{-1}$ ,  $1002.6 \text{ cm}^{-1}$  and  $942.3 \text{ cm}^{-1}$ .

The calculated torsional barrier of approximately  $1000 \text{ cm}^{-1}$  is much higher compared to that of the acetyl methyl group. A similar value was found for the propyl methyl group of methyl propyl ketone.<sup>[29]</sup> Comparing the microwave spectrum of MBK to that of methyl propyl ketone, we expect that splittings arising from the butyl methyl group are small, in the order of a few kHz, but resolvable with our experimental setup.

## 3. Microwave Spectrum

### 3.1. Rigid-Rotor Model

To assign the microwave spectrum of MBK, we first neglected the internal rotation effects and only considered the (00) species transitions predicted using the *XIAM* code<sup>[47]</sup> in its rigid-rotor mode. The rotational constants calculated at the

MP2/6-311++G(d,p) level of theory were taken as initial values (see Section 2.1.). We compared the experimental and the theoretical spectra predicted for all 11 conformers listed in Table 1, but all assignment attempts failed. Using the rotational constants from the B3LYP calculations as initial values did not improve the situation. Therefore, we suspected that the predicted rotational constants are not sufficiently accurate. This suspect was strongly supported by the same observation in our previous studies on methyl propyl ketone<sup>[29]</sup>, in which the alkyl group is one methylene group shorter than that of MBK. We assumed that, for methyl alkyl ketones, there was some kind of systematic errors in the calculations at the level of theory in use.

To quantify these errors, the relative deviations  $\Delta A$ ,  $\Delta B$ , and  $\Delta C$  in percent between the experimental rotational constants of methyl propyl ketone<sup>[29]</sup> and those predicted at different levels of theory in the basis set variation had been calculated (i.e.  $\Delta A = (A_{\text{cal}} - A_{\text{exp}})/A_{\text{exp}}$ ), and all values were averaged. In a next step, we came back to MBK and averaged the values of the rotational constants predicted at all levels of theory in Section 2.2., given in Table S3–S5. Lastly, we corrected the mean values of the rotational constants of MBK with the respective relative deviations obtained in the first step with the results from methyl propyl ketone by calculating  $A_{\text{MBK}} = \bar{A}_{\text{MBK}} \cdot 100 / (\bar{\Delta A}_{\text{MPK}} + 100)$ .  $B$  and  $C$  were calculated similarly.

This procedure was an attempt to compensate the errors in quantum chemical calculations at the used levels of theory, through which we obtained the rotational constants given in Table 1. These corrected rotational constants turned out to be surprisingly accurate, finally allowing the straightforward assignment of all three conformers.

### 3.2. One-Top Model

#### 3.2.1. Conformer I

As a next step, the internal rotation of the acetyl methyl group was considered. Here, an initial value for the torsional barrier is needed in the *XIAM* code. We first tried the values of  $147.6 \text{ cm}^{-1}$  and  $115.5 \text{ cm}^{-1}$  calculated at the MP2/6-311++G(d,p) and the B3LYP/6-311++G(d,p) level of theory, respectively (see Section 2.3.1.). However, the assignment of the (10) species transitions with these starting values turned out to be difficult, which led to the suspicion that they are not sufficiently accurate, either. In methyl propyl ketone<sup>[29]</sup>, we found a torsional barrier of  $188.3843(50) \text{ cm}^{-1}$  for the “pseudo- $C_s$ ” conformer. Trying this as initial value for conformer I of MBK led to a successful assignment. The initial values of the angles between the internal rotor axis  $i_1$  and the principal axes  $a$ ,  $b$ ,  $c$  are also needed. In contrast to the other initial parameters, the values calculated at the MP2/6-311++G(d,p) level of theory were sufficiently accurate. We note that the angle  $\alpha(i_1, c)$  could not be fitted and was fixed to  $90^\circ$ , a value which usually corresponds to a structure with an undistorted  $C_s$  symmetry.

Finally, 345 rotational transitions belonging to the (00) and (10) torsional states could be assigned to conformer I and fitted with the program *XIAM* (called Fit *XIAM(1Top)* in Table 3). The deduced barrier to the internal rotation of the acetyl methyl group is  $186.9198(50) \text{ cm}^{-1}$ , and the root-mean-square (rms) deviation of the fit is  $9.1 \text{ kHz}$ .

The experimental accuracy of the spectrometers for unblended lines is  $1-2 \text{ kHz}$ , as determined for carbonyl sulfide.<sup>[48]</sup> In the case of MBK, the resolution of a measured line can be much lower, for some transitions up to  $10 \text{ kHz}$  due to unresolved splittings of the butyl methyl rotor and additional spin-spin and spin-rotation couplings, which broaden the signals.

The average line width (FWHM) of about 35 kHz indicates a measurement accuracy of approximately 4 kHz. The rms deviation of the fit is thus more than twice the measurement accuracy. We noticed some systematic deviations of several branches (mainly *b*-type and forbidden *c*-type lines with  $K_a \geq 2$ ), where the experimental and predicted frequencies always differ by almost the same value of up to 30 kHz. This most likely indicates that one or several interaction terms are unaccounted for in the Hamiltonian.

The same set of data is refitted with the *BELGI-C<sub>s</sub>* program<sup>[49]</sup> in order to include higher order parameters. By floating 14 parameters, an rms deviation of 4.7 kHz was obtained. The barrier height is 186.7345(88)  $\text{cm}^{-1}$ . The *BELGI* parameters which can be transformed into the principal axis system are summarized in Table 3. The parameters in the original rho axis system are given in Table S8 in the SI. A list of the fitted frequencies along with their residuals obtained for both fits are available in Table S9 in the SI.

### 3.2.2. Conformer II

Conformer II possesses a  $C_1$  symmetry with the butyl group bent out of the C–(C=O)–C plane, where the  $\gamma$ -carbon is in a nearly synclinal position (see Section 2.1). Using the same strategy as that for conformer I, we tried to match conformer II of MBK with the  $C_1$  conformer of methyl propyl ketone, which has a similar structure.<sup>[29]</sup> The initial barrier to internal rotation of 238.14  $\text{cm}^{-1}$  was used. The assignment was straightforward. The 380 assigned torsional transitions were fitted in a *XIAM(1Top)* fit, yielding a torsional barrier of 233.5913(97)  $\text{cm}^{-1}$  (see Table 3). Although a few systematic deviations were observed, the *XIAM(1Top)* fit is quite satisfactory with an rms deviation of 3.9 kHz, which is within the measurement accuracy. The same 380 lines were refitted with the *BELGI-C<sub>1</sub>* code.<sup>[50]</sup> A fit with the same quality as the *XIAM(1Top)* fit was achieved by floating 16 parameters. The *BELGI* parameters in the rho axis system are given in Table S8 in the SI. The fitted frequencies along with their residuals obtained for both fits are listed in Table S10.

### 3.2.3. Conformer III

After conformer I and II were assigned, only transitions with medium or weak intensity remained in the broadband scan, which could be assigned to conformer III. According to calculations at the B3LYP/6-311++G(d,p) level of theory, this conformer is about 3–4  $\text{kJ}\cdot\text{mol}^{-1}$  higher in energy than conformer I and II (see Table 2). Therefore, only 234 transitions could be measured and fitted here. Conformer III shows a  $C_1$  structure, where the methyl group at the end of the butyl chain is in a synclinal position with respect to the C–(C=O)–C plane. Both, the *XIAM(1Top)* fit given in Table 3 and the *BELGI-C<sub>1</sub>* fit given in Table S8 in the SI, yield rms deviations within the measurement accuracy (3.0 kHz and 3.2 kHz, respectively). The fitted frequencies and their residuals obtained for both fits are listed in Table S11.

## 3.3. Two-Top Model

While the splittings between the (00) and (10) symmetry species arising from the internal rotation of the acetyl methyl group are clearly resolved in the broadband scan, additional splittings of the (00) species into the (00) and (01) species, as well as of the (10) species into the (10), (11) and (12) species, due to the internal rotation of the butyl methyl group, are small, ranging from only 100 kHz down to less than 2 kHz. Therefore, they are

only resolved in high resolution measurements and only in about half of the transitions. In the other half, they broaden the signals, as mentioned in Section 3.2.1. Figure 6 and 7 illustrate a typical spectrum of the  $5_{14} \leftarrow 4_{13}$  transition of conformer I with its clearly visible (10), (11) and (12) torsional components, while the splitting in (00) and (01) is not resolvable.

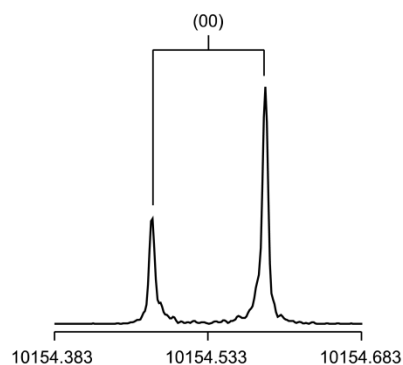


**Figure 6.** High resolution measurement of the  $5_{14} \leftarrow 4_{13}$  transition of conformer I. The (00) species is found at 10154.5331 MHz, while the splitting in the (00) and (01) species is not resolvable. The splitting indicated by the bracket is caused by the Doppler effect.

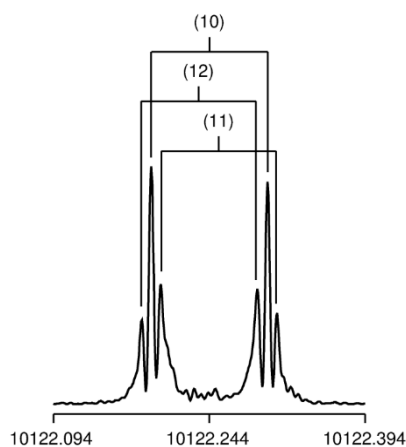


**Figure 7.** High resolution measurement of the  $5_{14} \leftarrow 4_{13}$  transition of conformer I. The (10), (11) and (12) species are found at 10122.2444 MHz, 10122.2530 MHz and 10122.2353 MHz, respectively. The splittings indicated by the brackets are caused by the Doppler effect.

We expanded the *XIAM(1Top)* fits described in Section 3.2. to the *XIAM(2Tops)* fits also given in Table 3 by including the (01), (11) and (12) torsional species of rotational transitions with resolvable splittings. The initial values for the barrier heights and the angles between the internal rotor axis  $i_2$  and the principal axes are taken from calculations at the MP2/6-311++G(d,p) level (see Table S1 in the SI). The total numbers of lines increase to 563 for conformer I, 555 for conformer II and 244 for conformer III. Only 10 new lines are added in the two-top fit of conformer III, which is due to the weak intensities of all its transitions.

The deduced barriers to internal rotation of the butyl methyl group of conformer I–III are 979.99(88)  $\text{cm}^{-1}$ , 1016.30(77)  $\text{cm}^{-1}$ , and 961.9(32)  $\text{cm}^{-1}$ , respectively. The values of all other fitted parameters are very similar to those of the one-top fits. The angles  $\alpha(i_2, g)$ , with  $g = a, b, c$ , could not be fitted and were fixed to the calculated values. The respective rms

deviation is 10.1 kHz, 5.1 kHz, and 3.3 kHz, which is always about 1 kHz higher than the value found for the corresponding one-top fit. There are two main reasons for this: 1) The measurement accuracy of the (01), (11) and (12) torsional transitions is lower than that of the (00) and (01) species, and 2) among the 15 fitted parameters, only one parameter, the  $V_3$  potential of the butyl methyl group, accounts for the (00)-(01) and (10)-(11)-(12) splittings.

To check for convergence, we carried out further *XIAM(2Tops)* fits where the relative frequencies  $\nu_{(01)} - \nu_{(00)}$ ,  $\nu_{(11)} - \nu_{(10)}$  and  $\nu_{(12)} - \nu_{(10)}$  instead of the absolute line frequencies, i.e. only the torsional splittings, were fitted. Here, only the  $V_3$  potential of the butyl methyl group was floated and all other parameter values, such as the rotational constants and the angles between the internal rotor axes and the inertial axes, were fixed to those of the *XIAM(1Top)* fit. The relative *XIAM* fit was only better in the case of conformer I with an rms deviation of 5.6 kHz. For conformers II and III, the deviations are 5.7 kHz and 5.1 kHz, respectively. The fitted frequencies and their residuals are given in Table S12 – S14 of the SI.

## 4. Discussion

We could assign all of the lines in the microwave spectrum of MBK to conformer I, II and III, except a few lines of extremely weak intensity, which might belong to impurities or  $^{13}\text{C}$  isotopologues. There are five major results: 1) Three conformers of MBK can be identified in the jet-cooled microwave spectrum. 2) Conformer I possesses a straight butyl chain. 3) Conformer II shows a  $C_1$  structure with the  $\gamma$ -carbon of the butyl group bent to a nearly synclinal position. 4) In conformer III, the methyl group at the end of the butyl chain is bent to a synclinal position. 5) The barrier heights of the acetyl methyl group deduced from the torsional splittings in the spectrum are  $186.9198(50) \text{ cm}^{-1}$ ,  $233.5913(97) \text{ cm}^{-1}$ , and  $182.2481(25) \text{ cm}^{-1}$  for conformer I, II, and III, respectively. The following sections will be divided in respective paragraphs giving detailed discussions on all of the statements above.

### 4.1. Geometries of the Three Observed Conformers

Only the energetically most favorable conformers are expected to be observed in the microwave spectrum under the measurement conditions described in the *Experimental Section*. From Section 2.1., we know that the order in energy of the conformers is very different in calculations with the MP2 and the B3LYP methods. The experimental rotational constants of the observed conformers clearly agree with those of the three lowest energy conformers calculated at the B3LYP/6-311++G(d,p) level of theory. Therefore, we conclude that for MBK, the energies calculated with DFT using the functional B3LYP are in better agreement with the experimental results. Including Grimme's dispersion correction does not significantly improve the agreement between the predicted and the experimental rotational constants.

Special attention should be paid to the structure of conformer I. Calculations at both, the MP2/6-311++G(d,p) and the B3LYP/6-311++G(d,p) level of theory, stated that not all heavy atoms are located on a symmetry plane ( $C_s$  structure), but the entire butyl group is slightly tilted out of the C-(C=O)-C plane ("pseudo- $C_s$ " structure) (see Section 2.1.). However, the *BELGI- $C_s$*  code, which is specially designed for a molecule with a plane of symmetry at equilibrium, could reproduce the

experimental data to measurement accuracy. Moreover, no  $c$ -type transitions were observed. This discrepancy confronts us with three possibilities for the structure of conformer I. First, the calculated  $C_1$  structure is correct, but due to a very small dipole moment component in  $c$  direction, the  $c$ -type transitions are too weak and cannot be observed. Second, the equilibrium structure is  $C_s$  and the calculations have failed to find the correct minima. Third, the enantiomers are separated by only a small barrier and the tunneling ground state lies above this barrier. In this case, the *effective* structure is  $C_s$ , the dipole moment in  $c$  direction would be zero and thus, no  $c$ -type transitions visible.

The potential energy curves for the acetyl methyl rotation illustrated in Figure 4 strongly support the last possibility. The height of the local maxima located in between the double minima is  $18.1 \text{ cm}^{-1}$  and  $1.4 \text{ cm}^{-1}$  calculated with the MP2 and the B3LYP method, respectively. The respective tunneling ground state is calculated to be  $29 \text{ cm}^{-1}$  and  $23 \text{ cm}^{-1}$ , clearly higher than the tunneling barrier. Another observation backing a  $C_s$  or *effective*  $C_s$  structure, is the inertial defect  $\Delta_c = I_c - I_a - I_b$  with an experimental value of approximately  $-16.00 \text{ u}\text{\AA}^2$ . If the heavy atom skeleton is planar and there are five pairs of out-of-plane hydrogens, the inertial defect is  $-15.60 \text{ u}\text{\AA}^2$ . The inertial defects obtained for the "pseudo- $C_s$ " structures calculated at the MP2/6-311++G(d,p) and the B3LYP/6-311++G(d,p) level of theory are  $-16.72 \text{ u}\text{\AA}^2$  and  $-15.76 \text{ u}\text{\AA}^2$ , respectively.

The symmetry of conformer II is  $C_1$  and contains the  $C_1$  conformer of methyl propyl ketone<sup>[29]</sup> as a sub-structure. This can also be observed for a series of microwave spectroscopic studies on  $n$ -alkyl acetates and methyl alkanoates.<sup>[1]-[8]</sup>

In case of conformer III, the butyl methyl group is bent to a synclinal position. The experimentally deduced rotational constants for this conformer are very similar to those of conformer II (see Table 3), which might complicate the distinction between those two. However, the angles between the internal rotor axis and the principal axes give helpful hints, because they are quite different for the two conformers ( $\alpha(i,a) = 44.78^\circ$ ,  $\alpha(i,b) = 45.54^\circ$ , and  $\alpha(i,c) = 85.78^\circ$  in the case of Conformer III and  $\alpha(i,a) = 155.92^\circ$ ,  $\alpha(i,b) = 100.18^\circ$ , and  $\alpha(i,c) = 68.42^\circ$  for Conformer II).

The experimental rotational constants obtained by the *XIAM(1Top)* fits agree within 1–2 % with the values calculated at different levels of theory (see Section 2.2.) for all three assigned conformers. Only the rotational constant  $A$  of conformer II is not calculated well with deviations of up to 5% at some level of theory using the MP2 method. It is interesting that the deviations between the experimental and predicted rotational constants are very similar to those found in methyl propyl ketone.<sup>[29]</sup> This seems to support our assumption given in Section 3.1. about some systematic errors in the quantum chemical calculations of linear methyl alkyl ketones, at least at the current levels of theory in use. The *BELGI* rotational constants are in agreement (within 1%) with the *XIAM* values, however, they do not agree within the standard errors. The most significant difference is that of the  $A$  rotational constant ( $\Delta \approx 15 \text{ MHz}$  in the case of conformer I). This is probably due to the different approaches used in *BELGI* and *XIAM*. While the *BELGI* program is a pure "rho axis method" code, the *XIAM* program uses a combined axis method, which is a combination of the principal axis method and the rho axis method. Furthermore, different sets of parameters are fitted, and the physical meaning of some parameters becomes less clear. Especially in the *BELGI* program, the  $A$  rotational constant is rather sensitive and can become an effective parameter in the fitting process. This is not

a seldom observation, as has been found in many previous studies with *BELGI-XIAM* comparisons, for example in ethyl methyl ketone ( $\Delta \approx 40$  MHz),<sup>[28]</sup> propyl methyl ketone ( $\Delta \approx 30$ –55 MHz),<sup>[29]</sup> ethyl acetate ( $\Delta \approx 40$  MHz),<sup>[4]</sup> vinyl acetate ( $\Delta \approx 25$  MHz),<sup>[51]</sup> and 4-hexyn-3-ol ( $\Delta \approx 35$  MHz).<sup>[52]</sup> This problem also occurs when *XIAM* is compared to other programs treating internal rotations, such as *ERHAM*,<sup>[53]</sup> for example in studies on methyl isobutyl ketone ( $\Delta \approx 8$  MHz)<sup>[24]</sup> and isopropenyl acetate ( $\Delta \approx 7$  MHz).<sup>[54]</sup>

#### 4.2. Torsional Barriers of the Acetyl Methyl Group

The acetyl methyl group of conformer I features a barrier to internal rotation of approximately  $180\text{ cm}^{-1}$ , while the value found for conformer II is about  $240\text{ cm}^{-1}$ . For the two conformers assigned in the microwave spectrum of methyl propyl ketone, the same observation with the respective values of  $188.3843(50)\text{ cm}^{-1}$  and  $238.145(21)\text{ cm}^{-1}$ , could be made.<sup>[29]</sup> In the literature, further ketones containing an acetyl methyl group have supported a classification for the barrier height of the acetyl methyl group in ketones, as illustrated in Figure 8. The first class comprises molecule with a  $C_1$  structure similar to that of conformer II of MBK, where the  $\gamma$ -carbon of the alkyl chain is tilt out of the C–(C=O)–C plane to a synclinal position (called the  $C_1$  class). The torsional barrier of the acetyl methyl group is always around  $240\text{ cm}^{-1}$ . Examples of this class are conformer II of MBK ( $233.5913(97)\text{ cm}^{-1}$ ), the  $C_1$  conformer of methyl propyl ketone ( $238.145(21)\text{ cm}^{-1}$ ),<sup>[29]</sup> allyl acetone ( $224.95(12)\text{ cm}^{-1}$ )<sup>[26]</sup> and methyl isobutyl ketone ( $250.3(19)\text{ cm}^{-1}$ ).<sup>[24]</sup> The second class includes ketones in which the torsional barrier of the acetyl methyl group is always around  $180\text{ cm}^{-1}$ , such as conformer I of MBK ( $186.9198(50)\text{ cm}^{-1}$ ), the  $C_s$  conformer of methyl propyl ketone ( $188.3843(50)\text{ cm}^{-1}$ ),<sup>[29]</sup> methyl ethyl ketone ( $183.1702(82)\text{ cm}^{-1}$ )<sup>[28]</sup> and methyl neopentyl ketone ( $174.11(27)\text{ cm}^{-1}$ ).<sup>[25]</sup> The “pseudo- $C_s$ ” structure seems to be responsible for this value. This class is thus called the  $C_s$  class.

Obviously, the barrier of about  $240\text{ cm}^{-1}$  found for the  $C_1$  structure is significantly higher than that linked to the “pseudo- $C_s$ ” structure, but the reason behind this is not obvious. One could argue that the  $C_1$  structure with the  $\gamma$ -carbon of the alkyl chain in a synclinal position would cause higher steric hindrance and consequently higher barriers. But if this argument were correct, the barrier height found in methyl neopentyl ketone, which possesses a highly branched alkyl chain (see Figure 8), should not be  $174.11(27)\text{ cm}^{-1}$ , but about  $240\text{ cm}^{-1}$ .<sup>[25]</sup> Therefore, we suspect that electronic effects have more influence on the acetyl methyl torsion than steric effects do. The electronic configuration on the other side of the carbonyl group is not the same in case of a  $C_s$  or *effective*  $C_s$  structure compared to a  $C_1$  structure.

The barrier height of  $182.2481(25)\text{ cm}^{-1}$  found for conformer III of MBK yields another key observation. Although this conformer has a  $C_1$  structure, it falls into the second class where all the molecules feature  $C_s$  symmetry. By looking at its potential energy curves given in Figure 5, there are double minimum potentials similar to those in the curves of conformer I in Figure 4 (see Section 2.3.1.). This kind of double minimum potentials has been reported in all molecules stated in the  $C_s$  class above. We thus conclude that the electrostatic interactions only stretch to the  $\gamma$ -carbon of the alkyl chain and not further.

To summarize, the torsional barrier of the acetyl methyl group is influenced by the configuration of the alkyl chain but only up to the  $\gamma$ -carbon. If the alkyl chain is “cut-off” at the  $\gamma$ -carbon and the “rest” features a “pseudo- $C_s$ ” structure, the barrier height is around  $180\text{ cm}^{-1}$ . If the “rest” is  $C_1$  symmetric,

the barrier height is approximately  $240\text{ cm}^{-1}$ . Further linear aliphatic ketones will be investigated in the near future to verify this “two-class” concept.

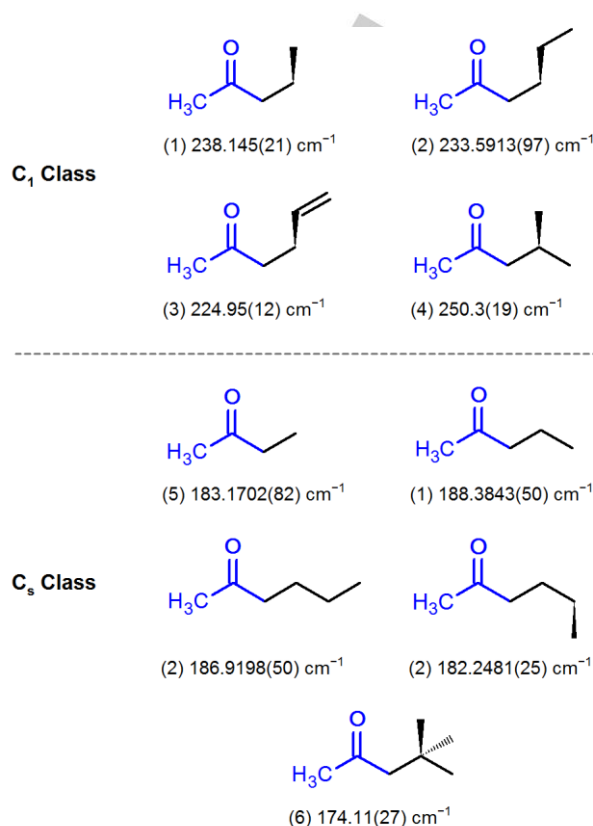


**Figure 8.** Experimental torsional barriers of the acetyl methyl group in different ketones: (1) methyl propyl ketone<sup>[29]</sup>, (2) MBK, (3) allyl acetone,<sup>[26]</sup> (4) methyl isobutyl ketone,<sup>[24]</sup> (5) methyl ethyl ketone,<sup>[28]</sup> and (9) methyl neopentyl ketone.<sup>[25]</sup>

Finally, we note that the simplest ketone containing an acetyl methyl group, acetone, is not considered in our comparison. The alkyl chain of acetone with only one methyl group is not long enough to support our classification into “pseudo- $C_s$ ” and  $C_1$ . Furthermore, the two equivalent methyl groups in acetone with their strong coupled LAM make this molecule a special case.<sup>[55,56]</sup>

There are also ketones which do not belong to either of the two classes mentioned above. For example, the high torsional barrier of the acetyl methyl group of methyl vinyl ketone is  $433.8(1)\text{ cm}^{-1}$  for the *ap* conformer and  $376.6(2)\text{ cm}^{-1}$  for the *sp* conformer,<sup>[15]</sup> probably because of mesomeric effects. If a bulky group is present at the other side of the carbonyl group, i.e. in cyclopropyl methyl ketone,<sup>[57]</sup> phenylacetone,<sup>[17]</sup> and acetovanillone,<sup>[58]</sup> as well as in  $\alpha$ -ionone and  $\beta$ -ionone,<sup>[59]</sup> different effects occurring from sterical hindrance cause the torsional barriers to range from about  $240\text{ cm}^{-1}$  to  $620\text{ cm}^{-1}$ . Further ketone studies are required to create a classification for these molecules.

## Conclusions

Three conformers of MBK were assigned in the jet-cooled microwave spectrum. Conformer I possesses a straight butyl chain, whereas conformer II shows a  $C_1$  structure with the butyl



group bent out of the C–(C=O)–C plane to a nearly synclinal position. In conformer III, the methyl group at the end of the butyl chain is in a synclinal position. The barriers heights of the acetyl methyl group deduced by fitting the torsional splittings in the spectrum with the program XIAM are 186.9198(50) cm<sup>-1</sup>, 233.5913(97) cm<sup>-1</sup>, and 182.2481(25) cm<sup>-1</sup> for conformer I, II, and III, respectively. The BELGI code was also used to fit the same data set and reduced the rms deviation to measurement accuracy. The barrier to internal rotation of the butyl methyl group could be deduced from the XIAM two-top fits to be about 1000 cm<sup>-1</sup> for all three conformers. The results serve as a milestone for a two-class concept linking the acetyl methyl torsional barrier to the conformational geometry, whereby electrostatic interactions from the alkyl chain seem to influence the acetyl methyl torsion, but only up to the  $\gamma$ -carbon. If the relevant parts of the alkyl chain show a “pseudo-C<sub>s</sub>” structure, the barrier height is approximately 180 cm<sup>-1</sup>, as found for conformer I and III. If the relevant part is C<sub>1</sub> symmetric, as in the case of conformer II, the barrier height is around 240 cm<sup>-1</sup>.

## Experimental Section

MBK was purchased from Alfa Aesar GmbH & Co KG, Karlsruhe, Germany with a stated purity of more than 98 % and no further purification steps were carried out. The sample was placed on a piece of pipe cleaner under a helium flow with a pressure of about 200 kPa. The helium-substance mixture was expanded through a pulsed nozzle into the vacuum chamber. A series of overlapping spectra from 9.0 to 14.6 GHz was recorded with a step size of 0.25 MHz using a modified version of the molecular jet Fourier transform microwave (MJ-FTMW) spectrometer described in ref. [60], which operates in a frequency range from 2.0 to 26.5 GHz. Afterwards, the transitions were measured or remeasured at high resolution, whereby a second MJ-FTMW spectrometer operating from 26.5 to 40.0 GHz<sup>[61]</sup> was used.

## Acknowledgements

This work was supported by the Agence Nationale de la Recherche ANR (project ID ANR-18-CE29-0011). Chloé Quignot is gratefully acknowledged for her contribution during her L2 research project at the Université Paris-Est Créteil. Simulations were performed with computing resources granted by RWTH Aachen University under project rwth0249, and the D3 calculations by Dr. Halima Mouhib.

**Keywords:** rotational spectroscopy • large amplitude motion • ab initio calculations • ketones • pheromones

- [1] H. V. L. Nguyen, I. Kleiner, S. T. Shipman, Y. Mae, K. Hirose, S. Hatanaka, K. Kobayashi, *J. Mol. Spectrosc.* **2014**, *299*, 17-21.
- [2] H. V. L. Nguyen, W. Stahl, I. Kleiner, *Mol. Phys.* **2012**, *110*, 2035-2042.
- [3] A. O. Hernandez-Castillo, C. Abeysekera, B. M. Hays, I. Kleiner, H. V. L. Nguyen, T. S. Zwier, *Mol. Phys.* **2012**, *110*, 2035-2042.
- [4] D. Jelisavac, D. C. Cortés Gómez, H. V. L. Nguyen, L. W. Sutikdja, W. Stahl, I. Kleiner, *J. Mol. Spectrosc.* **2009**, *257*, 111-115.
- [5] L. W. Sutikdja, W. Stahl, V. Sironneau, H. V. L. Nguyen, I. Kleiner, *Chem. Phys. Lett.* **2016**, *663*, 145-149.
- [6] T. Attig, L. W. Sutikdja, R. Kannengießer, I. Kleiner, W. Stahl, *J. Mol. Spectrosc.* **2013**, *284-285*, 8-15.
- [7] T. Attig, R. Kannengießer, I. Kleiner, W. Stahl, *J. Mol. Spectrosc.* **2013**, *290*, 24-30.
- [8] T. Attig, R. Kannengießer, I. Kleiner, W. Stahl, *J. Mol. Spectrosc.* **2014**, *298*, 47-53.
- [9] H. V. L. Nguyen, H. Mouhib, W. Stahl, I. Kleiner, *Mol. Phys.* **2010**, *108*, 763-770.
- [10] H. Mouhib, D. Jelisavac, W. Stahl, R. Wang, I. Kalf, U. Englert, *ChemPhysChem* **2011**, *12*, 761-764.
- [11] L. W. Sutikdja, D. Jelisavac, W. Stahl, I. Kleiner, *Mol. Phys.* **2012**, *110*, 2883-2893.
- [12] L. Evangelisti, L. B. Favero, A. Maris, S. Melandri, A. Vega-Toribio, A. Lesarri, W. Caminati, *J. Mol. Spectrosc.* **2010**, *259*, 65-69.
- [13] W. Caminati, J.-U. Grabow, *J. Am. Chem. Soc.* **2006**, *128*, 854-857.
- [14] L. Evangelisti, S. Tang, B. Velino, B. M. Giuliano, S. Melandri, W. Caminati, *Chem. Phys. Lett.* **2009**, *473*, 247-250.
- [15] D. S. Wilcox, A. J. Shirar, O. L. Williams, B. C. Dian, *Chem. Phys. Lett.* **2011**, *508*, 10-16.
- [16] M. Onda, Y. Kohama, K. Suga, I. Yamaguchi, *J. Mol. Struct.* **1998**, *442*, 19-22.
- [17] M. J. Tubergen, R. J. Lavrich, D. F. Plusquellic, R. D. Suenram, *J. Phys. Chem. A* **2006**, *110*, 13188-13194.
- [18] A. Maris, S. Melandri, W. Caminati, P. G. Favero, *Chem. Phys. Lett.* **1996**, *256*, 509-512.
- [19] S. Blanco, J. C. Lopez, A. B. Gomez, J. L. Alonso, *Mol. Phys.* **1999**, *97*, 853-858.
- [20] F. L. Bettens, R. P. A. Bettens, R. D. Brown, P. D. Godfrey, *J. Am. Chem. Soc.* **2000**, *122*, 5856-5860.
- [21] D. Loru, M. A. Bermúdez, M. E. Sanz, *J. Chem. Phys.* **2016**, *145*, 074311.
- [22] S. Melandri, A. Maris, B. M. Giuliano, W. Caminati, *J. Chem. Phys.* **2005**, *123*, 164304.
- [23] J. Gao, N. A. Seifert, W. Jäger, *Phys. Chem. Chem. Phys.* **2019**, Advance Article.
- [24] Y. Zhao, W. Stahl, H. V. L. Nguyen, *Chem. Phys. Lett.* **2012**, *545*, 9-13.
- [25] Y. Zhao, J. Jin, W. Stahl, I. Kleiner, *J. Mol. Spectrosc.* **2012**, *281*, 4-8.
- [26] L. Tulimat, H. Mouhib, I. Kleiner, W. Stahl, *J. Mol. Spectrosc.* **2015**, *312*, 46-50.
- [27] V. Van, W. Stahl, H. V. L. Nguyen, *Chem. Phys. Chem.* **2016**, *17*, 3223.
- [28] H. V. L. Nguyen, V. Van, W. Stahl, I. Kleiner, *J. Chem. Phys.* **2014**, *140*, 214303.
- [29] M. Andresen, I. Kleiner, M. Schwell, W. Stahl, H. V. L. Nguyen, *J. Phys. Chem. A* **2018**, *122*, 7071-7078.
- [30] J. B. Leikin, F. P. Paloucek in *Poisoning and Toxicology Handbook*, 4<sup>th</sup> Ed., Informa Healthcare USA, New York, **2008**, pp. 737.
- [31] D. Wittmann, G. Lübke, W. Francke, *Z. Naturforsch.* **1989**, *44c*, 325-326.
- [32] R. Boch, D. A. Shearer, *J. Insect. Physiol.* **1971**, *17*, 2277-2285.
- [33] H. J. Bestmann, O. Vostrowsky, *Chem. unserer Zeit* **1993**, *27*, 123-133.
- [34] W. Francke, G. Lübke, W. Schröder, A. Reckziegel, V. Imperatriz-Fonseca, A. Kleinert, E. Engels, K. Hartfelder, R. Radtke, W. Engels, *J. Braz. Chem. Soc.* **2000**, *11*, 562-571.
- [35] L. Ferres, J. Cheung, W. Stahl, H. V. L. Nguyen, *J. Phys. Chem. A* **2019**, DOI: 10.1021/acs.jpca.9b00029.
- [36] H. Dreizler, *Z. Naturforsch.* **1961**, *16a*, 1354-1367.
- [37] P. R. Bunker, P. Jensen in *Molecular Symmetry and Spectroscopy*, 2<sup>nd</sup> Ed., NRC Research Press: Ottawa, Ontario, Canada, **2006**.
- [38] M. J. Frisch, G. W. Trucks, H. B. Schlegel, G. E. Scuseria, M. A. Robb, J. R. Cheeseman, G. Scalmani, V. Barone, B. Mennucci, G. A. Petersson, H. Nakatsuji, M. Caricato, X. Li, H. P. Hratchian, A. F. Izmaylov, J. Bloino, G. Zheng, J. L. Sonnenberg, M. Hada, M. Ehara, K. Toyota, R. Fukuda, J. Hasegawa, M. Ishida, T. Nakajima, Y. Honda, O. Kitao, H. Nakai, T. Vreven, J. A. Montgomery, Jr., J. E. Peralta, F. Ogliaro, M. Bearpark, J. J. Heyd, E. Brothers, K. N. Kudin, V. N. Staroverov, R. Kobayashi, J. Normand, K. Raghavachari, A. Rendell, J. C. Burant, S. S. Iyengar, J. Tomasi, M. Cossi, N. Rega, J. M. Millam, M. Klene, J. E. Knox, J. B. Cross, V. Bakken, C. Adamo, J. Jaramillo, R. Gomperts, R. E. Stratmann, O. Yazyev, A. J. Austin, R. Cammi, C. Pomelli, J. W. Ochterski, R. L. Martin, K. Morokuma, V. G. Zakrzewski, G. A. Voth, P. Salvador, J. J. Dannenberg, S. Dapprich, A. D. Daniels, O. Farkas, J. B. Foresman, J. V. Ortiz, J. Cioslowski, D. J. Fox, Gaussian, Inc., Wallingford CT, **2009**.
- [39] E. G. Schnitzler, N. A. Seifert, S. Ghosh, J. Thomas, Y. Xu, W. Jäger, *Phys. Chem. Chem. Phys.* **2017**, *19*, 4440-4446.
- [40] M. E. Sanz, S. Blanco, J. C. López, J. L. Alonso, *Angew. Chem.* **2008**, *47*, 6216-6220.

- [41] P. Ottaviani, B. Velino, W. Caminati, *Chem. Phys. Lett.* **2006**, *428*, 236-240.
- [42] J.-R. A. Moreno, D. Petitprez, T. R. Huet, *Chem. Phys. Lett.* **2006**, *419*, 411-416.
- [43] H. V. L. Nguyen, W. Stahl, *Chem. Phys. Chem.* **2011**, *12*, 1900-1905.
- [44] Y. Zhao, H. V. L. Nguyen, W. Stahl, J. T. Hougen, *J. Mol. Spectrosc.* **2015**, *318*, 91-100.
- [45] E. Caldeweyher, C. Bannwarth, S. Grimme, *J. Chem. Phys.* **2017**, *147*, 034112.
- [46] W. Stahl, H. Dreizler, *Z. Naturforsch.* **1983**, *38a*, 1010-1014.
- [47] H. Hartwig, H. Dreizler, *Z. Naturforsch.* **1996**, *51a*, 923-932.
- [48] J.-U. Grabow, W. Stahl, *Z. Naturforsch.* **1990**, *45a*, 1043-1044.
- [49] J. T. Hougen, I. Kleiner, M. Godefroid, *J. Mol. Spectrosc.* **1994**, *163*, 559-586.
- [50] I. Kleiner, J. T. Hougen, *J. Chem. Phys.* **2003**, *119*, 5505-5509.
- [51] H. V. L. Nguyen, A. Jabri, V. Van, W. Stahl, *J. Phys. Chem. A* **2014**, *118*, 12130-12136.
- [52] K. Eibl, W. Stahl, I. Kleiner, H. V. L. Nguyen, *J. Chem. Phys.* **2018**, *149*, 144306.
- [53] P. Groner, *J. Chem. Phys.* **1997**, *107*, 4483-4498.
- [54] H. V. L. Nguyen, W. Stahl, *J. Mol. Spectrosc.* **2010**, *264*, 120-124.
- [55] V. V. Ilyushin, J. T. Hougen, *J. Mol. Spectrosc.* **2013**, *289*, 41-49.
- [56] P. Groner, S. Albert, E. Herbst, F. C. D. Lucia, F. J. Lovas, B. J. Drouin, J. C. Pearson, *Astrophys. J. Suppl.* **2002**, *142*, 145.
- [57] P. L. Lee, R. H. Schwendeman, *J. Mol. Spectrosc.* **1972**, *41*, 84-94.
- [58] E. J. Cocinero, F. J. Basterretxea, P. Écija, A. Lesarri, J. A. Fernández, F. Castaño, *Phys. Chem. Chem. Phys.* **2011**, *13*, 13310-13318.
- [59] I. Uriarte, S. Melandri, A. Maris, C. Calabrese, E. J. Cocinero, *J. Phys. Chem. Lett.* **2018**, *9*, 1497-1502.
- [60] J.-U. Grabow, W. Stahl, H. Dreizler, *Rev. Sci Instrum.* **1996**, *67*, 4072-4084.
- [61] I. Merke, W. Stahl, H. Dreizler, *Z. Naturforsch.* **1994**, *49a*, 490-496.

## Entry for the Table of Contents (Please choose one layout)

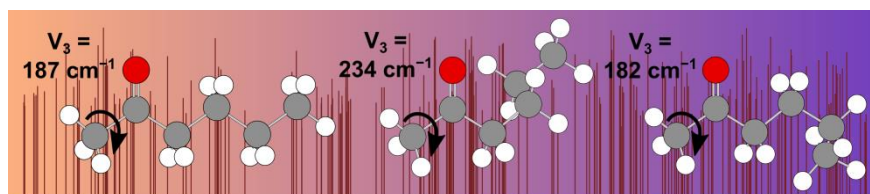
Layout 2:

## FULL PAPER

Maike Andresen, Isabelle Kleiner, Martin Schwell, Wolfgang Stahl, Ha Vinh Lam Nguyen\*

Page No. – Page No.

Sensing the Molecular Structures of Hexan-2-one by Internal Rotation and Microwave Spectroscopy



A combination of quantum chemistry and microwave spectroscopy was used to analyze the gas-phase structures of hexan-2-one. The barrier heights of the acetyl methyl group could be linked to the conformational structures and a rule to predict the torsional barrier was deduced.

**Table 1.** Relative energies with (ZPE) and without (E) zero-point corrections (in  $\text{kJ}\cdot\text{mol}^{-1}$ ), rotational constants (in GHz), dipole moment components (in Debye) and dihedral angles (in degree) of the eleven stable conformers of methyl butyl ketone calculated at the MP2/6-311++G(d,p) level of theory.

	$E^{[a]}$	ZPE <sup>[b]</sup>	A	B	C	$ \mu_a $	$ \mu_b $	$ \mu_c $	$\theta_1$	$\theta_2$	$\theta_3$
II	0.00	0.00	5.573	1.259	1.181	0.66	2.96	1.08	161.2	-70.3	179.6
VI	1.86	2.60	4.426	1.339	1.323	1.89	2.01	2.20	58.6	59.9	178.3
X	1.89	3.41	3.844	1.741	1.514	0.59	3.41	0.08	64.0	55.0	59.0
I	2.10	1.35	7.439	1.041	0.942	0.26	3.30	0.08	169.4	178.8	179.7
V	2.17	2.78	4.133	1.532	1.432	0.25	2.34	2.07	159.8	-64.8	-59.4
IX	3.56	4.32	3.934	1.682	1.544	0.02	1.23	2.90	156.6	-84.8	58.6
III	3.83	3.53	5.780	1.189	1.047	1.10	3.00	0.67	171.1	174.0	62.8
IV	4.11	4.43	6.184	1.074	0.994	2.58	2.26	1.35	61.0	175.8	179.7
VIII	5.34	6.26	5.615	1.179	1.109	2.70	2.53	0.07	60.7	171.9	62.3
VII	6.41	7.15	5.549	1.222	1.071	1.96	3.02	0.80	62.8	-179.7	-63.2
XI	7.75	8.87	3.547	1.749	1.604	1.73	2.08	2.29	54.5	74.7	-69.6
Exp. I <sup>[c]</sup>			7.511	1.041	0.941	7.510 <sup>[d]</sup>	1.040 <sup>[d]</sup>	0.941 <sup>[d]</sup>			
Exp. II <sup>[c]</sup>			5.865	1.244	1.153	5.856 <sup>[d]</sup>	1.243 <sup>[d]</sup>	1.151 <sup>[d]</sup>			
Exp. III <sup>[c]</sup>			5.848	1.174	1.052	5.849 <sup>[d]</sup>	1.176 <sup>[d]</sup>	1.045 <sup>[d]</sup>			

<sup>[a]</sup> Referring to the absolute energy of  $E = -310.243919$  Hartree of conformer II. <sup>[b]</sup> Referring to the zero-point corrected energy of  $E = -310.072583$  Hartree of conformer II. <sup>[c]</sup> Experimentally deduced rotational constants. <sup>[d]</sup> Corrected rotational constants A, B, and C of the respective conformer, see Section 3.1.

**Table 2.** Relative energies with (ZPE) and without (E) zero-point corrections (in  $\text{kJ}\cdot\text{mol}^{-1}$ ), rotational constants (in GHz), dipole moment components (in Debye) and dihedral angles (in degree) of the eleven stable conformers of methyl butyl ketone calculated at the B3LYP/6-311++G(d,p) level of theory.

	$E^{[a]}$	ZPE <sup>[b]</sup>	A	B	C	$ \mu_a $	$ \mu_b $	$ \mu_c $	$\theta_1$	$\theta_2$	$\theta_3$
I	0.00	0.00	7.526	1.029	0.932	0.29	2.92	0.05	174.5	179.0	-179.9
II	0.67	1.38	5.818	1.219	1.138	0.56	2.67	0.83	166.2	-72.9	-179.6
III	3.34	3.62	5.850	1.161	1.032	1.00	2.62	0.65	173.1	175.2	65.8
IV	4.27	5.52	6.273	1.054	0.976	2.32	2.03	1.13	61.2	177.1	-179.8
V	4.67	5.58	4.494	1.394	1.313	0.24	2.38	1.38	166.6	-72.0	-67.0
VI	5.55	6.80	4.566	1.282	1.254	1.81	1.81	1.84	56.8	63.7	178.4
VII	6.65	8.20	5.743	1.172	1.069	1.37	2.72	0.86	91.8	-178.1	-65.3
VIII	7.46	8.73	5.628	1.156	1.084	2.47	2.19	0.11	62.2	175.1	65.8
IX	7.76	8.74	4.042	1.576	1.452	0.03	1.43	2.42	161.2	-89.1	62.7
X	8.54	10.34	4.031	1.585	1.397	0.69	3.03	0.16	64.2	60.1	62.8
XI	12.70	14.14	3.576	1.676	1.545	1.59	1.83	2.06	54.3	76.2	-69.6
Exp. I <sup>[c]</sup>			7.511	1.041	0.941	7.510 <sup>[d]</sup>	1.040 <sup>[d]</sup>	0.941 <sup>[d]</sup>			
Exp. II <sup>[c]</sup>			5.865	1.244	1.153	5.856 <sup>[d]</sup>	1.243 <sup>[d]</sup>	1.151 <sup>[d]</sup>			
Exp. III <sup>[c]</sup>			5.848	1.174	1.052	5.849 <sup>[d]</sup>	1.176 <sup>[d]</sup>	1.045 <sup>[d]</sup>			

<sup>[a]</sup> Referring to the absolute energy of  $E = -311.191516$  Hartree of conformer II. <sup>[b]</sup> Referring to the zero-point corrected energy of  $E = -311.023059$  Hartree of conformer II. <sup>[c]</sup> Experimentally deduced rotational constants. <sup>[d]</sup> Corrected rotational constants A, B, and C of the respective conformer, see Section 3.1.

**Table 3.** Molecular parameters of conformer I, II and III of methyl butyl ketone obtained from the *XIAM* code taking into account the internal rotation of the acetyl methyl group (fits *XIAM(1Top)*) and of both, the acetyl and the butyl methyl group (fits *XIAM(2Tops)*). The parameters refer to the principal axis system and I' representation. Watson's A reduction was used. For conformer I the parameters of the *BELGI-C<sub>s</sub>* fit obtained by a transformation from the rho axis system into the principal axis are given.

Parameter	Conformer I			Conformer II		Conformer III	
	<i>BELGI-C<sub>s</sub></i>	<i>XIAM(1Top)</i>	<i>XIAM(2Tops)</i> <sup>[a]</sup>	<i>XIAM(1Top)</i>	<i>XIAM(2Tops)</i> <sup>[b]</sup>	<i>XIAM(1Top)</i>	<i>XIAM(2Tops)</i> <sup>[c]</sup>
<i>A</i> / GHz	7.49638(12)	7.5105223(12)	7.5105234(11)	5.86481492(70)	5.86481387(83)	5.84751340(35)	5.84751308(37)
<i>B</i> / GHz	1.040928(18)	1.04073147(13)	1.04073552(13)	1.24437761(10)	1.24438046(12)	1.173774262(80)	1.173775010(86)
<i>C</i> / GHz	0.9417953(20)	0.94131724(11)	0.94131348(11)	1.153435232(67)	1.153432435(79)	1.052431415(64)	1.052430622(69)
$\Delta_J$ / kHz	0.0449(03)	0.04753(56)	0.04792(53)	0.32050(26)	0.32060(28)	0.15184(31)	0.15193(34)
$\Delta_{JK}$ / kHz		0.4780(26)	0.4814(23)	-3.4257(21)	-3.4241(24)	0.0739(25)	0.0733(27)
$\Delta_K$ / kHz		4.398(44)	4.469(39)	34.696(13)	34.672(14)	7.455(20)	7.457(21)
$\delta_J$ / kHz		0.004861(96)	0.004995(81)	-0.00179(15)	-0.00199(18)	0.01555(18)	0.01555(19)
$\delta_K$ / kHz				2.527(13)	2.541(15)	2.342(19)	2.342(20)
$F_{0,1}$ / GHz	158.183(24)	158.0(fixed)	158.0(fixed)	158.0(fixed)	158.0(fixed)	158.0(fixed)	158.0(fixed)
$V_{3,1}$ / cm <sup>-1</sup>	186.7345(88)	186.9198(50)	187.2303(49)	233.5913(97)	233.911(12)	182.2481(25)	182.2581(27)
$\angle(i,a)$ / °	148.2790(37)	148.2603(61)	148.2461(60)	155.930(15)	155.919(18)	44.7760(22)	44.7760(23)
$\angle(i,b)$ / °	121.7210(37)	121.7397(61)	121.7539(60)	100.153(52)	100.182(61)	45.5353(30)	45.5350(31)
$\angle(i,c)$ / °	90.00(fixed)	90.00(fixed)	90.00(fixed)	68.420(37)	68.424(44)	85.7736(55)	85.7750(60)
$D_{pi2,1}$ / MHz		0.02863(26)	0.02852(24)	0.22964(33)	0.22972(40)	0.03565(12)	0.03563(12)
$D_{pi2,-1}$ / MHz		-1.0209(50)	-1.0315(48)	-4.8637(54)	-4.8699(63)	-0.5510(13)	-0.5510(14)
$V_{3,2}$ / cm <sup>-1</sup>		0.00773(13)	0.00772(10)	0.14245(36)	0.14270(41)	0.00795(11)	0.00791(11)
$N$ <sup>[d]</sup>	345	345	563	380	555	234	244
$N_1$ <sup>[e]</sup>	144/201	144/201	144/201	196/184	196/184	139/95	139/95
$N_2$ <sup>[f]</sup>			32/94/92		13/81/81		0/5/5
$\sigma$ <sup>[g]</sup> / kHz	4.7	9.1	10.1	3.9	5.1	3.0	3.3

<sup>[a]</sup> For conformer I the internal rotation parameters of the second rotor are fixed to  $F_{0,2} = 158.0$  GHz,  $\angle(i_2,a) = 35.81^\circ$ ,  $\angle(i_2,b) = 54.19^\circ$ , and  $\angle(i_2,c) = 90.00^\circ$ . <sup>[b]</sup> For conformer II,  $F_{0,2} = 158.0$  GHz,  $\angle(i_2,a) = 20.61^\circ$ ,  $\angle(i_2,b) = 105.90^\circ$ , and  $\angle(i_2,c) = 102.77^\circ$ . <sup>[c]</sup> For conformer III,  $F_{0,2} = 158.0$  GHz,  $\angle(i_2,a) = 112.58^\circ$ ,  $\angle(i_2,b) = 39.82^\circ$ , and  $\angle(i_2,c) = 120.83^\circ$ . <sup>[d]</sup> Total number of lines. <sup>[e]</sup> Number of the (00)/(10) torsional transitions, respectively. <sup>[f]</sup> Number of the (01)/(11)/(12) torsional transitions, respectively. <sup>[g]</sup> Root-mean-square deviation of the fit.